Front. Earth Sci. 2017, 11(1): 95–113
DOI 10.1007/s11707-016-0580-5

RESEARCH ARTICLE

Projected hydrologic regime changes in the Poyang Lake Basin due to climate change

Le Wang, Shenglian Guo (✉), Xingjun Hong, Dedi Liu, Lihua Xiong

State key Laboratory of Water Resources and Hydropower Engineering Science, Wuhan University, Wuhan 430072, China

Abstract Poyang Lake, the largest freshwater lake in China, and its surrounding sub-basins have suffered frequent floods and droughts in recent decades. To better understand and quantitatively assess hydrological impacts of climate change in the region, this study adopted the Statistical Downscaling Model (SDSM) to downscale the outputs of a Global Climate Model (GCM) under three scenarios (RCP2.6, RCP4.5 and RCP8.5) as recommended by the fifth phase of the Coupled Model Inter-comparison Project (CMIP5) during future periods (2010−2099) in the Poyang Lake Basin. A semi-distributed two-parameter monthly water balance model was also used to simulate and predict projected changes of runoff in the Ganjiang sub-basin. Results indicate that: 1) SDSM can simulate monthly mean precipitation reasonably well, while a bias correction procedure should be applied to downscaled extreme precipitation indices (EPI) before being employed to simulate future precipitation; 2) for annual mean precipitation, a mixed pattern of positive or negative changes are detected in the entire basin, with a slightly higher or lower trend in the 2020s and 2050s, with a consistent increase in the 2080s; 3) all six EPI show a general increase under RCP4.5 and RCP8.5 scenarios, while a mixed pattern of positive and negative changes is detected for most indices under the RCP2.6 scenario; and 4) the future runoff in the Ganjiang sub-basin shows an overall decreasing trend for all periods but the 2080s under the RCP8.5 scenario when runoff is more sensitive to changes in precipitation than evaporation.

Keywords climate change, hydrological regimes, statistical downscaling, extreme precipitation indices, Poyang Lake Basin

Received July 27, 2015; accepted January 3, 2016

E-mail: slguo@whu.edu.cn

1 Introduction

The increased concentration of greenhouse gases since the preindustrial era has led to global warming, which is likely to cause intense and profound changes for both natural and social systems globally. Temperature, precipitation, and water vapor patterns are predicted to change significantly by the end of the 21st century (Houghton et al., 2001; IPCC, 2013). Rising global surface temperature is likely to change atmospheric circulation and accelerate the hydrological cycle (Houghton et al., 2001; Bates et al.,2008). The altered hydrological regimes will in turn affect almost every aspect of human activities. Thus, projecting future climate change and assessing its potential effects on hydrology and water resources remains a hot topic in recent hydrological research.

Over the past few decades many studies focusing on the impacts of climate change on hydrological regimes have been conducted. Many review articles have reported the general procedure for assessing these impacts (e.g., Xu 1999; Xu et al., 2005). Middelkoop et al. (2001) developed a water balance model to assess the impact of climate change on the river flow conditions in the Rhine basin. Shabalova et al. (2003) analyzed the change in the flow regime of the Rhine River by the end of the 21st century using both the Hadley Centre regional climate model (HadRM2) and a distributed hydrological model. Merritt et al. (2006) used outputs of three Global Circulation Models (GCMs) (CGCM2, CSIROMk2, and HadCM3) under two emissions scenarios (SRES A2 and B2) to drive the UBC Watershed Model to evaluate hydrologic response to climate change in sub-watersheds of the Okanagan Basin, British Columbia. Christensen and Lettenmaier (2007) suggested a multi-model ensemble approach to assess climate change impacts on the hydrology and water resources of the Colorado River Basin, in which outputs of 11 GCMs were combined to drive a VIC model. Raje and Krishnan (2012) used the Bayesian parameter uncertainty modeling approach in a

macro-scale hydrologic model to investigate the impact of climate change on the hydrological regimes of a river basin in India. These studies usually used a three-step process consisting of: 1) selecting appropriate GCMs under different greenhouse gas emission scenarios; 2) downscaling the GCM outputs to obtain finer-resolution climate variables (e.g., temperature and precipitation); and 3) using a hydrological model with the downscaled finer-resolution climate variables as inputs to simulate changes in the hydrological regimes at basin and regional scales.

Most of the previous studies that assessed climate change impacts on hydrological processes were based on IPCC SRES outputs (e.g., Middelkoop et al., 2001; Arnell, 2003; Chen et al., 2007; Fowler et al., 2007; Gosling et al., 2011; Islam et al., 2014). Nevertheless, a suite of Representative Concentration Pathways (RCPs) (Moss et al., 2010) has been developed for the Fifth Assessment Report (AR5) of the Intergovernmental Panel on Climate Change (IPCC, 2013). For the fifth phase of the Coupled Model Inter-comparison Project (CMIP5), four RCPs (RCP2.6, RCP4.5, RCP6.0 and RCP8.5) have been formulated based on a range of projections of future population growth, technological development, and societal responses. The labels for the RCPs provide a rough estimate of the radiative forcing in the year 2100 (relative to pre-industrial conditions) (Taylor et al., 2012) which could increase the understanding and awareness of scholars and policymakers about future climate change trends. Much attention has recently been given to utilizing CMIP5 data at different scales-global or regional. Alkama et al. (2013) used observations and simulations from CMIP5 models to investigate changes in global streamflow, and found that most models could simulate streamflow reasonably well, with the exception of South America and Africa. Sillmann et al. (2013) analyzed the projected climate extremes indices from a CMIP5 multi-model ensemble at global and regional scales during the 21st century. Aich et al. (2014) compared impacts of climate change on streamflow in four large African river basins using a hydrological model with outputs from CMIP5 models. Thibeault and Seth (2014) evaluated projected climate extremes indices in the northeast United States using gridded observations and 23 CMIP5 coupled models. Huang et al. (2014) reported changes in the annual precipitation projected by multiple CMIP5 models over central Asia in the 21st century. Li et al. (2015) analyzed joint probability behaviors of precipitation extremes in China during 2021–2050 and 2071–2100 under historical and RCP2.6 and RCP8.5 scenarios from CMIP5 datasets. However, research on hydrological responses to climate change based on RCP scenarios in China remains limited (Wang et al., 2014).

Poyang Lake, the largest freshwater lake in China and located in a critical area in the middle of the Yangtze River Basin (Kanai et al., 2002), is well known for its ecological and economic importance. It is a type of wetland with high biodiversity, flood storage function, and sustainability of water supply services under climate change (Zhang et al., 2011a). However, the lake and its surrounding sub-basins have suffered frequent floods and droughts in recent decades. Consequently, an increasing number of studies have reported on climate change impacts on the variability of precipitation regimes in this area (Ye et al., 2011; Sun et al., 2014; Tao et al., 2014; Zhang et al., 2014a; Ye et al., 2015). Zhang et al. (2011b) investigated probability behavior and trends of flow extremes (the 7-day high flow) and found that increasing precipitation intensity and more frequent rainstorms might intensify flood events across the Poyang Lake Basin. Zhang et al. (2011a) analyzed changing precipitation and associated impacts on hydrological processes of the basin and seasonal transitions of precipitation were observed. However, most previous studies focused on an increased understanding of the hydrological mechanisms from the past few decades. Studies of future projections of hydrological regimes in the region are still insufficient.

Recognizing the above concerns, this paper attempts to investigate the impacts of future climate change on hydrological regimes based on a one-way coupling of a GCM and a simple hydrological model through the statistical downscaling model (SDSM) in the Poyang Lake Basin. The specific objectives of this study include: 1) evaluating the applicability of the SDSM in simulating mean precipitation and EPI; 2) investigating the projected changes of precipitation (mean and extreme events) under future emission scenarios by using projections of a GCM (BCC-CSM1.1) downscaled by the calibrated SDSM; and 3) assessing hydrological changes for future periods (2010–2099) by using the downscaled future climate change scenarios and the calibrated hydrological model. The results are expected to not only provide an important scientific basis for local water resources management, flood protection, and drought mitigation in the Poyang Lake Basin, but also provide a reference for similar studies in other regions of the world.

2 Study area and data

Poyang Lake lies in the center of the Yangtze River Basin, between 28°22′N –29°45′N and 115°47′E –116°45′E, and accounts for 9% of the total drainage area at 162,225 km^2 (Fig. 1). The lake's primary source of water inflow is received from five rivers (Ganjiang, Fuhe, Xinjiang, Raohe, and Xiushui) and discharges into the Yangtze River from a narrow outlet in the north. In this study, the Poyang Lake Basin (PYLB) was divided into six sub-basins: Xiushui (XS), Ganjiang (GJ), Fuhe (FH), Xinjiang (XJ), Raohe (RH), and Poyang Lake (PYL) (Fig. 1).

The climate of PYLB is subtropical monsoon, and the topography varies from highly mountainous and hilly (maximum elevation of about 2200 m above the sea level)

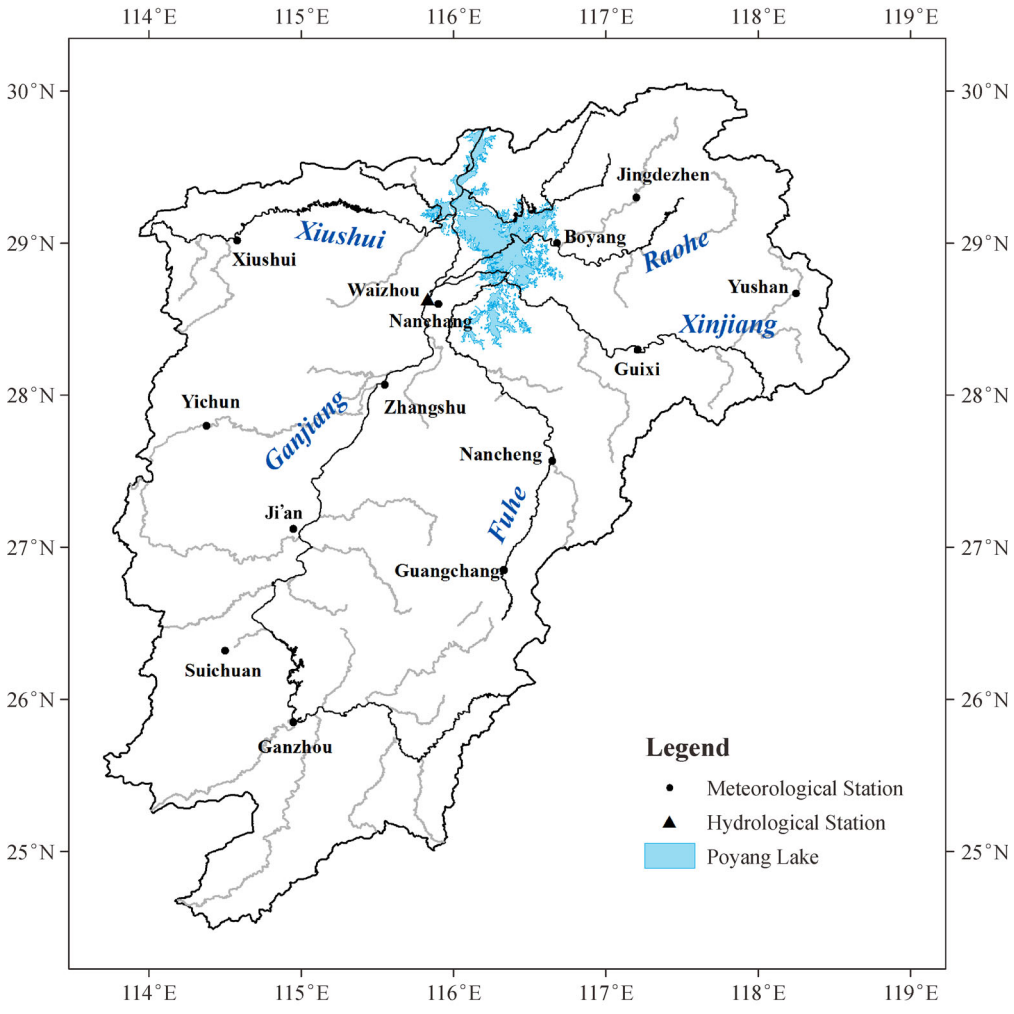

Fig. 1 Geographical locations of the main rivers and hydro-meteorological stations in the Poyang Lake Basin

to alluvial plains in the lower reaches of the primary watercourses (Ye et al., 2011). Water inputs into the Poyang Lake from the five sub-basins are particularly important during the wet season from April to June when heavy rainfall produces large surface flows from the sub-basins to the lake (Shankman et al., 2006).

Observed daily precipitation data from 13 meteorological stations (Table 1) in the PYLB from 1961 to 2005 were obtained from the China Meteorological Data Sharing Service System (http://cdc.cma.gov.cn/index.jsp). These stations are evenly distributed over the PYLB (Fig. 1). In addition, observed monthly precipitation, temperature, pan evaporation, and streamflow data (at Waizhou Station) in the Ganjiang sub-basin from 1961 to 2005 were accessed to calibrate the hydrological model, with 1961−1990 as the calibration period and 1991−2005 as the verification period.

3 Methods

3.1 BCC-CSM1.1 model

The BCC-CSM1.1 model, developed by the Beijing Climate Center in China, was chosen for this study due to its good performance in reproducing observed climate variations of temperature and precipitation in China in recent decades (Xin et al., 2013). Three scenarios (RCP2.6, RCP4.5, and RCP8.5), representing low, moderate, and high emission scenarios, respectively, were used. Different large-scale atmospheric variables, which were further screened for selecting suitable predictors, were derived from the daily reanalysis dataset of the National Center for Environmental Prediction (NCEP) (http://www.esrl.noaa.gov/psd/) for 1961−2005, as well as outputs of the BCC-CSM1.1 model under three scenarios from 1961 to 2099,

representing the current and future climate scenarios, respectively. The future periods were divided into three parts: 2020s (2010–2039), 2050s (2040–2069), and 2080s (2070–2099). The simulations of historical periods (1961–2005) of the BCC-CSM1.1 model served as a reference for future projection and changes.

3.2 Statistical downscaling model (SDSM)

Since spatial resolutions of GCM grids are often too coarse to resolve many important sub-grid scale processes, there is a mismatch of scale between GCM outputs and the scale of interest for regional or local applications. In order to deal with the problem of spatial scale mismatch, different downscaling methods have been proposed and widely used in the past few decades (Wilks 1989; Hellström et al., 2001; Hanssen et al., 2005; Wetterhall et al., 2006; Chu et al., 2010).

Downscaling methods are generally divided into two categories: dynamic downscaling and statistical downscaling. The sstatistical downscaling method aims to derive appropriate statistical or empirical relationships, which can transform large-scale atmospheric features (predictors) to local-scale or station-scale variables (predictands), such as precipitation and temperature. Statistical downscaling methods are effective to fill the gap between large-scale climate change and local-scale hydrological response (Chu et al., 2010).

The SDSM model (Wilby et al., 1999,2002) is a hybrid of a stochastic weather generator and multi-linear regression method. Many comparative studies (Wilby et al., 1998; Dibike and Coulibaly, 2005; Harpham and Wilby, 2005; Khan et al., 2006) have shown that this model is simple to use and has performed well (Chu et al., 2010), and therefore has been widely employed in climate change impact assessments. The formulations of SDSM are briefly described as follows (Wilby et al., 1999,2003;Wetterhall et al., 2006):

First, large-scale atmospheric predictors are used to condition the precipitation occurrence and to calculate the precipitation amount on wet days, i.e.,

$$\omega_t = \alpha_0 + \sum_{j=1}^{n} \alpha_j \hat{u}_t{}^{(j)} + \alpha_{t-1}\omega_{t-1}, \tag{1}$$

where t represents time (days), n is the number of the selected predictor, ω_t and ω_{t-1} are the conditional possibilities of precipitation occurrence on day t and day t−1, respectively, $\hat{u}_t^{(j)}$ is the normalized predictor, α_0 and α_j are regression parameters determined by the least square method, and α_{t-1} is a lag−1 day regression parameter. It is emphasized that ω_{t-1} and α_{t-1} are optional, depending on the study region and predictand. A uniformly distributed random number $r_t(0 \leqslant r_t \leqslant 1)$ is used to determine the precipitation occurrence and it is assumed that rain would happen if $\omega_t \leqslant r_t$.

On a wet day, precipitation can be expressed by a z-score as:

$$Z_t = \beta_0 + \sum_{j=1}^{n} \beta_j \hat{u}_t{}^{(j)} + \beta_{t-1} Z_{t-1} + \varepsilon, \tag{2}$$

where Z_t and Z_{t-1} are the z-scores on day t and day t−1, respectively, β_0, β_j, and β_{t-1} are regression parameters, with β_{t-1} and Z_{t-1} optional. ε is a random error term simulated by the normal distribution $N(0,\sigma_\varepsilon^2)$.

Second, the amount of precipitation y_t on day t can be simulated as:

$$y_t = F^{-1}[\phi(Z_t)], \tag{3}$$

where ϕ is the normal cumulative distribution function and F is the empirical distribution function of y_t.

3.3 Extreme precipitation indices (EPI)

Extreme precipitation events can be defined in different ways, such as large areas experiencing unusual precipitation values over longer periods of time, or the impact such an event could have on society (e.g., a number of mortalities, excessive economic or monetary losses, or both). However, these definitions are all qualitative descriptions. Developing a suite of extreme precipitation indices that combine quantitative measurements is essential (Easterling et al., 2000).

Until now, various EPI have been proposed and applied for different research needs. A series of key indices of climate extremes, with 31 EPI included, were developed by the European Union STARDEX (STAtistical and Regional dynamical Downscaling of EXtremes for European regions) project. The Expert Team on Climate Change Detection, Monitoring and Indices (ETCCDMI) also proposed a comprehensive list of indices including 11 EPI, accompanied by definitions, procedures, and guidance for large-scale regional studies. In addition, Frich et al. (2002) recommended five EPIs which were used to measure extreme precipitation. As numerous precipitation indices have been used in previous studies of climate extremes (Plummer et al., 1999; Peterson et al., 2002; Sen Roy and Balling, 2004), Qian and Lin (2005) suggested that an EPI should include three characteristics: magnitude, intensity, and persistence. To address this need, in this study six EPI representing these three characteristics were selected from the ETCCDMI list (Table 2), of which two indices (R95p and R90N) relate to precipitation magnitude, two indices (Rx5day and SDII) describe precipitation intensity, and two indices (CDD and CWD) demonstrate precipitation persistence. These yearly EPI were calculated using the computer program RClimDex. Developed and maintained by Zhang and Yang (2004) at the Climate Research Branch of Meteorological Service of Canada,

Table 1 List of 13 meteorological stations with mean annual temperature and precipitation during 1961–2005 in the Poyang Lake Basin

Station	Station code	Latitude (N)	Longitude (E)	Altitude/m	Temperature/°C	Precipitation/mm
Xiushui	57598	29°02′	114°35′	146.8	16.7	1583
Yichun	57793	27°48′	114°23′	131.3	17.3	1612
Ji'an	57799	27°03′	114°55′	71.2	18.5	1502
Suichuan	57896	26°20′	114°30′	126.1	18.6	1446
Ganzhou	57993	25°52′	115°00′	137.5	19.5	1433
Boyang	58519	29°00′	116°41′	40.1	17.8	1612
Jingdezhen	58527	29°18′	117°12′	61.5	17.5	1778
Nanchang	58606	28°36′	115°55′	46.9	17.7	1596
Zhangshu	58608	28°04′	115°33′	30.4	17.8	1637
Guixi	58626	28°18′	117°13′	51.2	18.4	1864
Yushan	58634	28°41′	118°15′	116.3	17.6	1823
Nancheng	58715	27°35′	116°39′	80.8	17.9	1681
Guangchang	58813	26°51′	116°20′	143.8	18.3	1728

Table 2 Extreme precipitation indices

Category	Index	Unit	Definition
Precipitation percentile	R95p	mm	Total amounts of precipitation > long-term 95th percentile of daily precipitation during a year
	R90N	d	No. of events > long-term 90th percentile
Precipitation intensity	Rx5day	mm	Greatest 5-day total rainfall per year
	SDII	mm/d	Simple daily intensity index (total rainfall/total rain-day per year)
Precipitation persistence	CDD	d	Maximum number of consecutive dry days
	CWD	d	Maximum number of consecutive wet days

RClimDex includes a user-friendly software package that is freely available online to the international research community (http://cccma.seos.uvic.ca/ETCCDI/). It also provides comprehensive descriptions of these indices, details of quality control procedures, and references to relevant literature.

3.4 Two-Parameter Monthly Water Balance Model (TPWBM)

During the past few decades, many hydrological models have been developed and used for different hydrological purposes including flood forecasting, water resources assessment, impact of climate and land use change, streamflow generation in ungauged basins, and so on (Refsgaard et al., 1988; Widén-Nilsson et al., 2007; Jie et al., 2016). There has been a trend to develop complex models with a high degree of physical dependence and structural complexity for catchment studies. However, such models lead to increasing difficulty in estimating parameters (Butts et al., 2004). Furthermore, large uncertainty exists in climate models and downscaling techniques, and the accuracy of climate change scenarios used to drive hydrological models is still limited at finer spatial and temporal scales. Therefore, simple models are typically used to investigate the hydrological impact of climate change.

The two-parameter monthly water balance model (TPWBM) was proposed and developed by Xiong and Guo (1999). The model has been tested in 100 small and medium sized basins in China and has been found to be comparable to more complex water balance models. Due to its simplicity and efficiency, the TPWBM was used in this study to investigate climate change impacts (Guo et al., 2002). The formulation of TPWBM is as follows.

Actual monthly evapotranspiration $E(t)$ is calculated by

$$E(t) = C \times EP(t) \times \tanh(P(t)/EP(t)), \quad (4)$$

where $EP(t)$ is the monthly pan evaporation, $P(t)$ is the monthly precipitation, and C is a model parameter.

Monthly runoff $Q(t)$ is assumed as a hyperbolic tangent function of the soil water content $S(t)$, which is given as

$$Q(t) = S(t) \times \tanh(S(t)/SC), \quad (5)$$

where SC is the field capacity of the basin and is the second model parameter.

Given the observation series of both the monthly precipitation $P(t)$ and the monthly pan evaporation

$EP(t)$, the actual monthly evapotranspiration $E(t)$ can be determined by Eq. (4). The quantity of the remaining water in the soil will be $[S(t-1)+P(t)-E(t)]$, after the loss of evapotranspiration$E(t)$, with $S(t-1)$ being the water content at the end of the month $t-1$ and at the beginning of the month t. Eq. (5) is then used to calculate the monthly runoff at month t, as follows

$$Q(t) = (S(t-1)+P(t)-E(t)) \times \tanh((S(t-1) + P(t)-E(t))/SC). \quad (6)$$

Finally, the water content $S(t)$ at the end of t^{th} month is calculated according to the water balance equation

$$S(t) = S(t-1)+P(t)-E(t)-Q(t). \quad (7)$$

4 Results and discussion

4.1 Calibrating and validating SDSM

The selection of suitable predictors is essential to establishment of SDSM, which requires that the predictors and predictands are physically linked, strongly correlated, and have a consistent relationship. Numerous studies (Dibike and Coulibaly, 2005; Harpham and Wilby, 2005; Chu et al., 2010; Chen et al., 2012; Guo et al., 2012, 2013) have been conducted on the screening of the most relevant predictors, which indirectly sets up an alternative ensemble of various atmospheric variables. In this study, the procedure for identifying suitable predictors was as follows: First, all available atmospheric variables were adopted as potential predictors (Chu et al., 2010; Guo et al., 2012). Second, the seasonal and partial correlation methods (Guo et al., 2012) were employed with the significance level of 0.05, in order to identify the most relevant predictors for each predictand (precipitation and temperature). Finally, considering parsimony and significance, six large-scale atmosphere variables were selected as the predictors for all stations: 850 hPa specific humidity (hus), 850 hPa air temperature (ta), 500 hPa eastward wind (ua), 500 hPa geopotential height (zg), sea level pressure (psl), and near-surface air temperature (tas). These variables were derived from the daily NCEP reanalysis dataset for 1961–2005, as well as outputs of BCC-CSM1.1 under each of the three RCP scenarios from 1961 to 2099, representing the current and future climate scenarios, respectively.

To evaluate the applicability of the SDSM model for simulating mean precipitation and selected extreme precipitation indices, SDSM must be calibrated and validated before downscaling precipitation with GCM predictors. The data series were divided into a calibration period (1961–1990) and a verification period (1991–2005). Figure 2 compares the NCEP/GCMs simulated and observed mean monthly precipitation in all sub-basins during the calibration period, showing the capability of SDSM for downscaling monthly precipitation in the Poyang Lake Basin. Since extreme climate events potentially have a much greater impact on water resources management than average values, it is necessary to assess the capacity of SDSM to simulate the characteristics of extreme precipitation events.

Figure 3 shows the simulation performance of SDSM for the selected EPI (results for the validation period are not given). The values of EPI are presented as box-and-whisker plots showing the median (cross), 25th and 75th percentiles (box), and 10th and 90th percentiles (whisker). The X axis labels denote all sub-basins and the whole basin. The box-and-whiskers in each sub-basin represent the observed, NCEP data, and GCM output simulations in turn. The comparison of EPI between the first (observation), second (NCEP simulation), and third (GCM output simulation) box-and-whiskers in Fig. 3 shows that the indices are not equally well modeled. The SDSM simulation underestimates R95p, Rx5day, CDD and CWD, and overestimates SDII in this region. For R90N, the NCEP and GCMs simulations fit well with the observed data. In addition, the simulated results for some EPI (R95p, R90N, Rx5day, and SDII) have narrower ranges than the observed EPI. The common narrower ranges show that the simulation results do not satisfactorily represent the variances for EPI, which makes it a challenge for the SDSM method to perform better in reproducing extreme precipitation events. We also note that simulated EPI biases from the NCEP data are less than those from the GCM output.

The above calibration results indicate the SDSM's limited capacity to represent extreme precipitation events, and a defect of stochastic precipitation models must be resolved (Teutschbein and Seibert, 2010). To account for this limitation, results require bias correction (Maraun et al., 2010) ,which is critical given climate models often provide biased representations of observed times series due to systematic model errors (Teutschbein and Seibert, 2010).

Typical bias correction methods are based on a stationary assumption that the same bias correction procedure and parameters apply to both control and scenario conditions, and generally aim at preserved mean values and standard deviation. For a detailed and comprehensive comparative study of bias-correction methods, we refer readers to Teutschbein and Seibert (2010). In this study, the method proposed by Hong et al. (2014) was used to correct the precipitation indices, as follows:

$$Ind_{t,bc} = \eta Ind_{t,sim} + \varphi, \quad (8)$$

where $Ind_{t,sim}$ and $Ind_{t,bc}$ are annual index series before and after bias correction at year t, respectively, and η and ϕ are

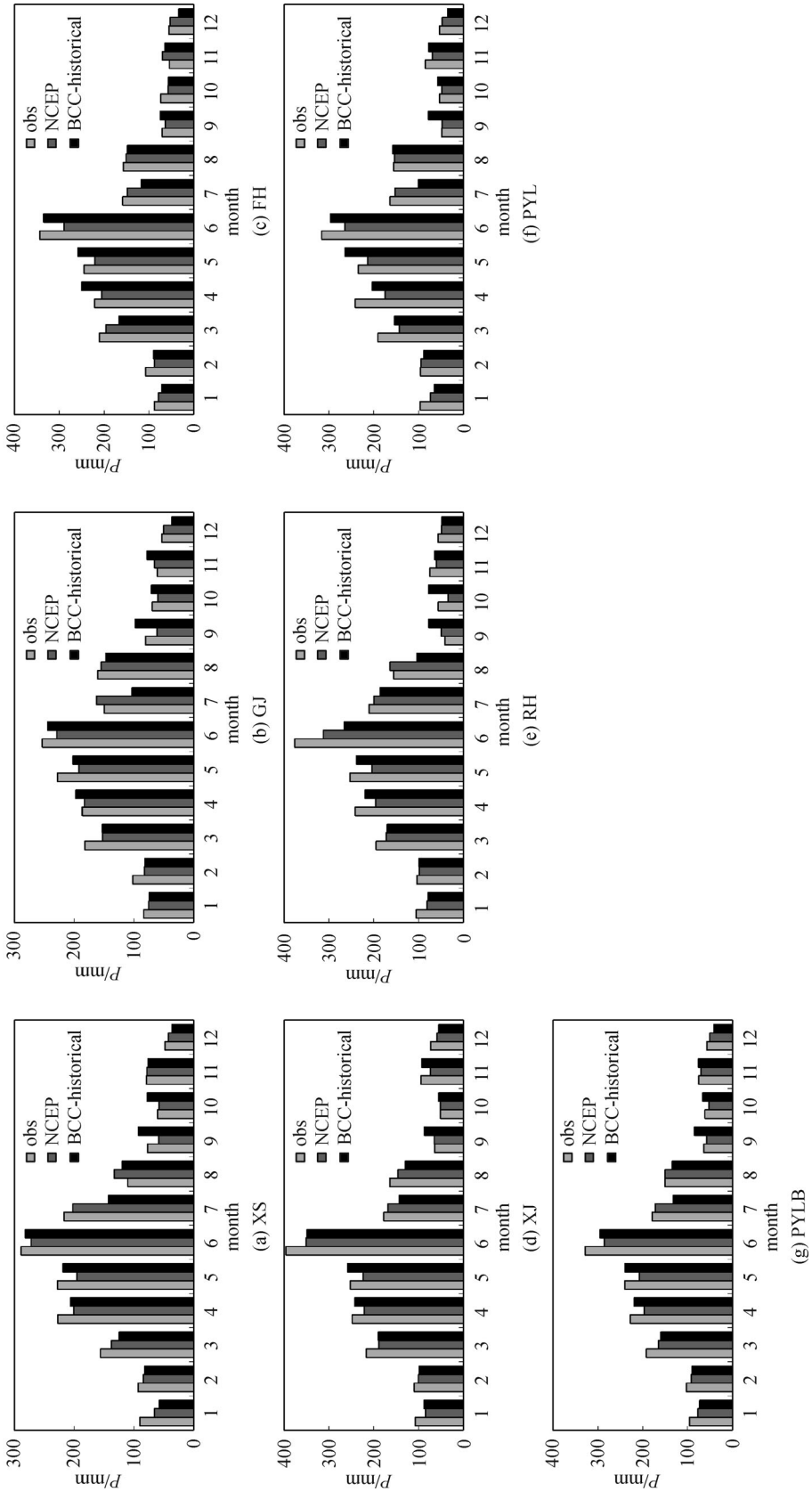

Fig. 2 Comparison of observed and simulated precipitation indices with NCEP and historical BCC-CSM1.1 output during calibration period (1961–1990) for each sub-basin and Poyang Lake Basin

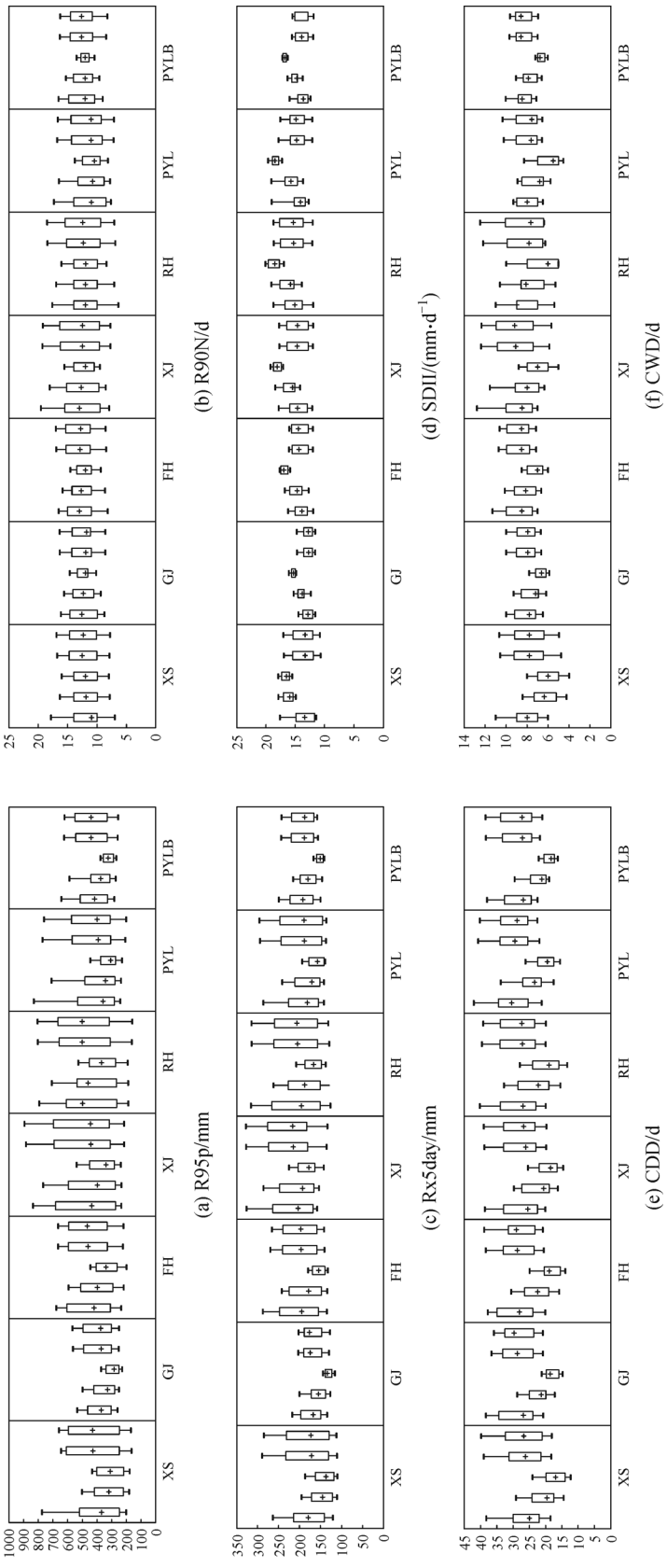

Fig. 3 Comparison of observed and simulated extreme precipitation indices using NCEP and historical BCC-CSM1.1 output during calibration period (1961–1990) for each sub-basin and Poyang Lake Basin. The first box-and-whisker in each sub-basin represents the observed EPI, the second and third represents EPI of NCEP data and GCM output simulations before bias-correction, and the fourth and fifth represent EPI of NCEP data and GCM output simulations after bias-correction.

correction factors of the variance and mean values. The latter are calculated as follows:

$$\eta = SD_{obs,his}/SD_{sim,his}, \quad (9)$$

$$\varphi = Ave_{obs,his} - \eta Ave_{sim,his}, \quad (10)$$

where $SD_{obs,his}$ and $SD_{sim,his}$ are standard deviation values of the observed and simulated annual index series during the historical period, and $Ave_{obs,his}$ and $Ave_{sim,his}$ are mean values of the observed and simulated annual index series during the historical period.

Results of EPI after bias correction were separately plotted as the fourth (NCEP simulations) and fifth (GCM output simulations) box-and-whiskers in Fig. 3. Compared to the second and third box-and-whiskers, statistical characteristics of simulated EPI series are closer to those of the observed values after the bias-correction. Therefore, after bias-correction, the SDSM model can be applied to represent future extreme precipitation events with climate projections.

4.2 Downscaling precipitation under future emission scenarios

The validated SDSM after bias-correction was used to downscale the large-scale predictor variables derived from the RCP2.6, RCP4.5, and RCP8.5 scenarios of BCC-CSM1.1, with daily precipitation simulated for the following periods: historical (1961–2005), 2020s (2010–2039), 2050s (2040–2069), and 2080s (2070–2099). The historical simulation acts as a reference for future projection and changes.

Projected changes in annual mean precipitation during future periods (2020s, 2050s, and 2080s) in the Poyang Lake Basin are shown in Table 3, showing a mixed pattern of positive or negative changes, with different (slightly higher or lower) trends in the 2020s and 2050s, and consistent with the increases in the 2080s. A significant increase was primarily found in the northeastern region (Raohe sub-basin and Poyang Lake) throughout the last 90 years. A decreasing trend was predominant in the southern region (Ganjiang and Fuhe sub-basins). In the Ganjiang sub-basin, a decrease in annual mean precipitation was observed in the 2020s and 2050s, followed by a minimal increase in the 2080s under the RCP2.6 and RCP4.5 scenarios. Ongoing changes during future periods are projected under the RCP8.5 scenario, with an 8.6% increase by the end of 21st century. The Fuhe sub-basin shows an overall descending trend for the next 90 years, with the greatest tendencies for future flooding observed for the Raohe sub-basin. For all sub-basins, the increase or decrease ranges are more pronounced under the RCP8.5 scenario than those of the RCP2.6 and RCP4.5 scenarios.

Climate change not only alters the average values, but also the frequency and intensity of extreme events. The latter are likely to exert a much greater impact on extremes than on mean climate values (Xu et al., 2009). An understanding of spatial and temporal patterns of extreme precipitation events in the future is of great importance for managing floods and droughts (Li et al., 2013; Zhang et al., 2014b). Figure 4 illustrates the changes of the selected EPI values during future periods, relative to the historical simulation under the three scenarios (RCP2.6, RCP4.5, and RCP8.5) in the Poyang Lake Basin.

All six EPIs generally increase for the whole basin under

Table 3 Projected future changes of annual mean precipitation in the Poyang Lake Basin

Sub-basin	Variable	RCP2.6				RCP4.5				RCP8.5			
		Base periods	2020s	2050s	2080s	Base periods	2020s	2050s	2080s	Base periods	2020s	2050s	2080s
XS	P(mm)	1922.1	1877.0	1865.4	1948.6	1922.1	1948.3	1900.5	1920.7	1922.1	1918.7	1935.3	1791.6
	$\Delta P/P$(%)	/	−2.3	−2.9	1.4	/	1.4	−1.1	−0.1	/	−0.2	0.7	−6.8
GJ	P(mm)	1538.2	1506.0	1495.4	1535.6	1538.2	1524.4	1517.0	1557.3	1538.2	1543.4	1546.9	1670.6
	$\Delta P/P$(%)	/	−2.1	−2.8	−0.2	/	−0.9	−1.4	1.2	/	0.3	0.6	8.6
FH	P(mm)	2067.0	2016.4	1967.2	2093.3	2067.0	2032.5	1886.3	1948.5	2067.0	1991.8	1968.1	1846.5
	$\Delta P/P$(%)	/	−2.4	−4.8	1.3	/	−1.7	−8.7	−5.7	/	−3.6	−4.8	−10.7
XJ	P(mm)	2236.8	2223.6	2227.4	2244.3	2236.8	2244.3	2164.7	2284.8	2236.8	2200.7	2163.4	2238.2
	$\Delta P/P$(%)	/	−0.6	−0.4	0.3	/	0.3	−3.2	2.1	/	−1.6	−3.3	0.1
RH	P(mm)	2147.0	2193.6	2237.0	2242.5	2147.0	2247.3	2189.0	2334.8	2147.0	2162.3	2233.7	2291.2
	$\Delta P/P$(%)	/	2.2	4.2	4.4	/	4.7	2.0	8.7	/	0.7	4.0	6.7
PYL	P(mm)	1799.7	1786.8	1842.8	1834.4	1799.7	1901.4	1901.2	1889.1	1799.7	1855.9	1941.0	1922.1
	$\Delta P/P$(%)	/	−0.7	2.4	1.9	/	5.7	5.6	5.0	/	3.1	7.8	6.8
PYLB	P(mm)	1846.6	1823.3	1823.2	1866.5	1846.6	1864.0	1818.4	1873.6	1846.6	1843.1	1854.4	1883.5
	$\Delta P/P$(%)	/	−1.3	−1.3	1.1	/	0.9	−1.5	1.5	/	−0.2	0.4	2.0

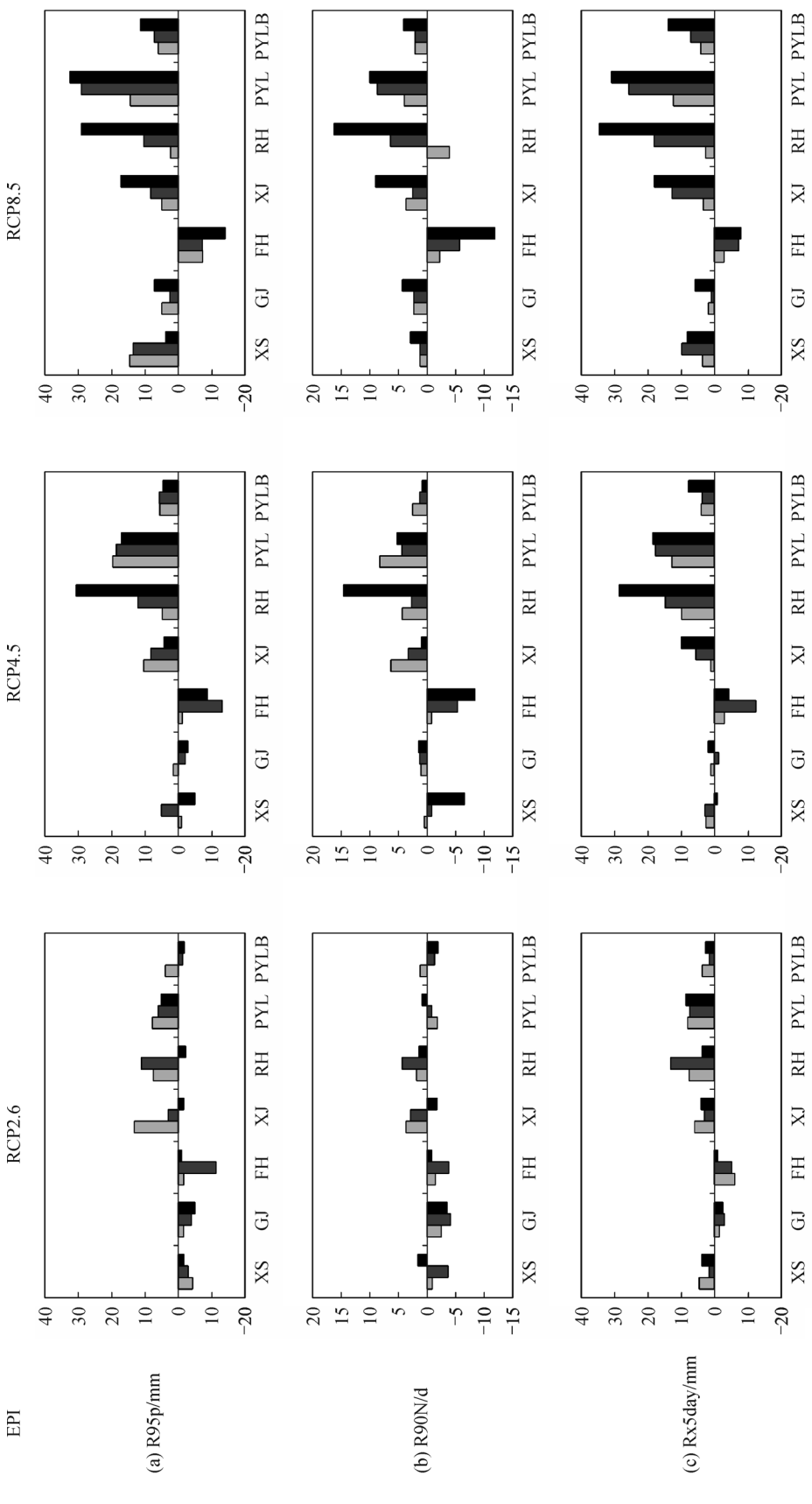
EPI
RCP2.6
RCP4.5
RCP8.5
(a) R95p/mm
(b) R90N/d
(c) Rx5day/mm
XS GJ FH XJ RH PYL PYLB

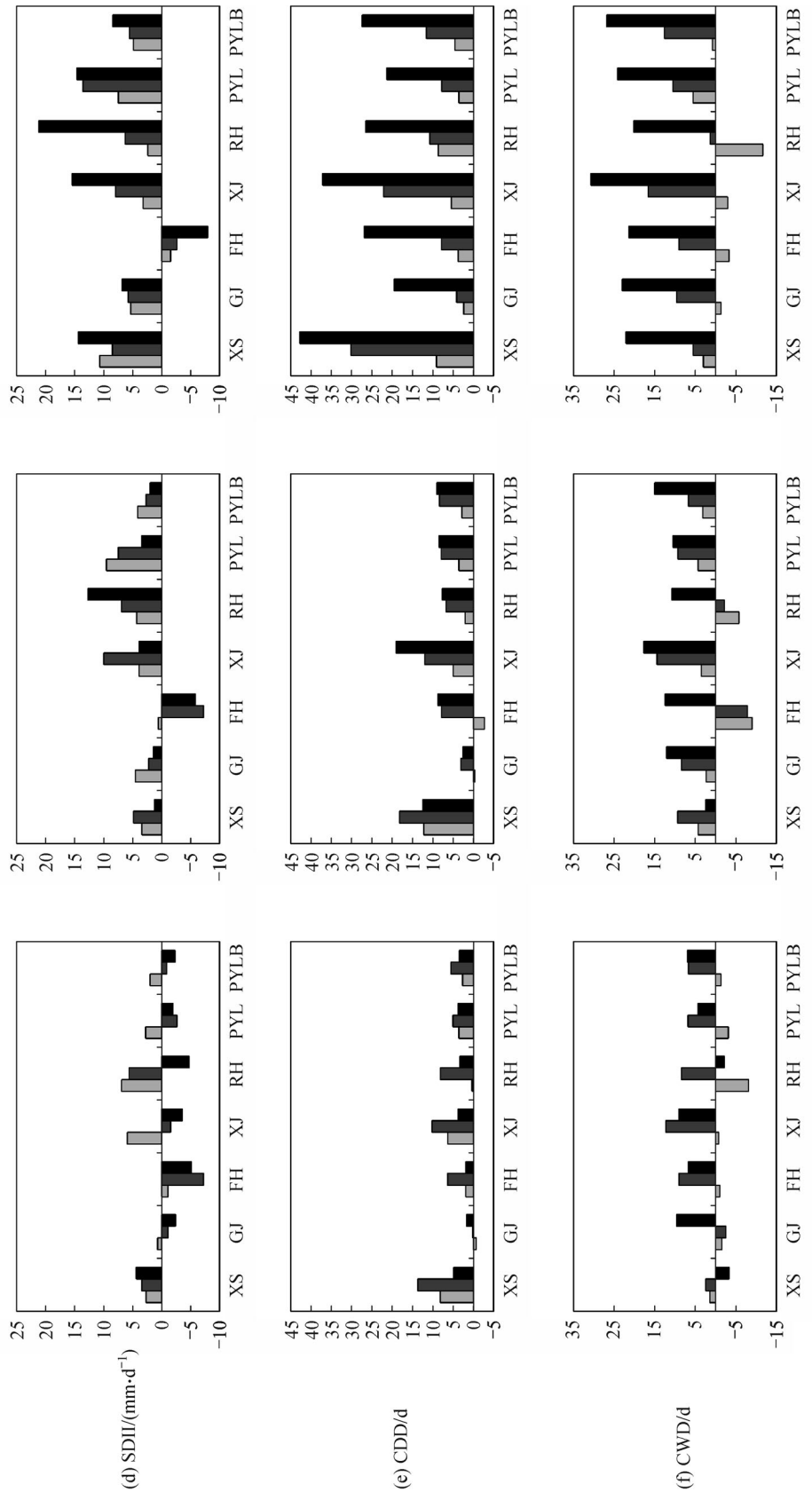

Fig. 4 Relative change in extreme precipitation indices (EPI) in the future period (2010–2099) at each sub-basin and the Poyang Lake Basin. Three histograms in each sub-basin represent future change in EPI during 2020s, 2050s, and 2080s, respectively, relative to the historical periods (1961–2005).

the RCP4.5 and RCP8.5 scenarios, both of which increase and decrease for most indices under the RCP2.6 scenario.

The changes with the R95p (Fig. 4(a)) and R90N (Fig. 4(b)) indices represent extreme precipitation percentiles, showing consistency under three scenarios in the whole basin. Under the RCP2.6 scenario, the temporal evolution of R95p and R90N first shows an increase in the 2020s, subsequently decreasing to below the base period level in the 2050s and 2080s, while a continuous increasing trend is seen under the RCP4.5 and RCP8.5 scenarios. The discrepancy suggests that the magnitude of extreme precipitation tends to increase as emission scenarios become more severe. P95p and R90N are predicted to substantially increase in the Poyang Lake and surrounding sub-basins in the east (Xinjiang and Raohe sub-basins), but only slightly increase and decrease in the western sub-basins (Xiushui and Ganjiang). By the end of the century, the growth of P95q in some sub-basins, such as Raohe sub-basin and Poyang Lake, can reach 30%, indicating a greater frequency of future occurrences of floods in the area.

As shown in Fig. 4(c), Rx5day demonstrates an overall increase in most sub-basins throughout the last 90 years, with the exception of a decrease of less than 5% in the Ganjiang sub-basin under the RCP2.6 scenario, and less than 15% in the Fuhe sub-basin under all scenarios. The greatest increases can be found in the Raohe sub-basin and Poyang Lake, which is above 30% in the 2080s. As an indicator of flood-producing events, the future Rx5day increases gradually over the Poyang Lake Basin, which pose a threat to the safety of flood control in the basin.

A general increase of SDII in Fig. 4(d) is projected in this study area under the RCP4.5 and RCP8.5 scenarios, except for the Fuhe sub-basin. Under the RCP2.6 scenario, the temporal evolution of SDII of most sub-basins first shows an increase in the 2020s, followed by a decrease to below the base period level. Overall, there is a trend of centralized precipitation in the entire Poyang Lake Basin.

CDD and CWD (Figs. 4(e) and 4(f)) indicate extreme precipitation persistence, with CDD relating to drought and CWD relating to flood. CDD is the only index that shows an overall increasing trend in each sub-basin under all scenarios; the Xiushui sub-basin has the largest increased value of 43%. Projected increases of CDD in the future are extremely high in all sub-basins under the RCP8.5 scenario, indicating greater risks of consecutive dry days, which would be challenging to water resource management in this region. Meanwhile, CWD is predicted to slightly decrease in the 2020s, with a more significant increase in the latter 21st century. For example, an increase of approximately 20%–30% is found in all sub-basins by the end-of-century under the RCP8.5 scenario. By contrast with CDD and other indices, the study area will probably experience more sudden changes from droughts to floods in the future under high representative concentration pathways.

4.3 Projected changes of runoff

Changes in precipitation and temperature will impact the hydrological cycle and cause temporal and spatial variations of runoff. Therefore, changes in runoff need to be simulated and predicted.

Ganjiang is the largest river in the Poyang Lake Basin (Fig. 1) and contributes almost 55% of the total discharge into the Poyang Lake (Shankman et al., 2006). It has also been the focus of flood control and drought mitigation in recent decades (Ye et al., 2013). These features make the Ganjiang sub-basin a suitable site for evaluating and predicting streamflow responses to climate change.

The Ganjiang sub-basin was divided into 129 grids, with each grid measuring 900 km^2 (30 km×30 km). The standard parameterization procedures for calibrating TPWBM can be found in Guo et al. (2002). TPWBM was calibrated and validated with observed flow data from 1961 to 2005 at Waizhou Station in the Ganjiang sub-basin, with 1961−1990 as the calibration period and 1991−2005 as the verification period. The value of Nash-Sutcliffe efficiency criterion and the relative error of the volumetric fit during calibration and verification periods are 0.84 and −4.86%, and 0.79 and −6.99%, respectively. Observed and simulated monthly runoff during the calibration and verification period is shown in Fig. 5. The simulated monthly runoff fits well with the observed data, which shows that the validated semi-distributed TPWBM model is efficient and useful in the monthly runoff simulation, and thus can be employed to simulate future runoff responses to climate change in the Ganjiang sub-basin.

The validated SDSM with bias correction was employed to downscale the large-scale climate variables of BCC-CSM1.1 under three scenarios, in order to derive watershed-scale hydrological variables (precipitation and temperature). Since the future evaporation data cannot be directly measured, it is commonly calculated using evaporation estimation methods based on climatic data, varying from simple empirical formulations (e.g., Thornthwaite 1948; Priestley and Taylor, 1972) to complex physically-based methods (e.g., Penman, 1948). However, complex methods usually require large amounts of meteorological data, e.g., wind speed and solar radiation, which are not easily obtained. Therefore, temperature-based methods, which require only air temperature as input data, are suggested in practice (Xu et al., 2001). Scatter diagrams of observed monthly pan evaporation and monthly mean air temperature are shown in Fig. 6. The monthly pan evaporation $EP(t)$ is an approximately exponential function of monthly mean air temperature $T(t)$, which is given as

$$EP(t) = A \times \exp(B \times T(t)), \tag{11}$$

where A and B are coefficients determined by the least square method. The regression analysis results between

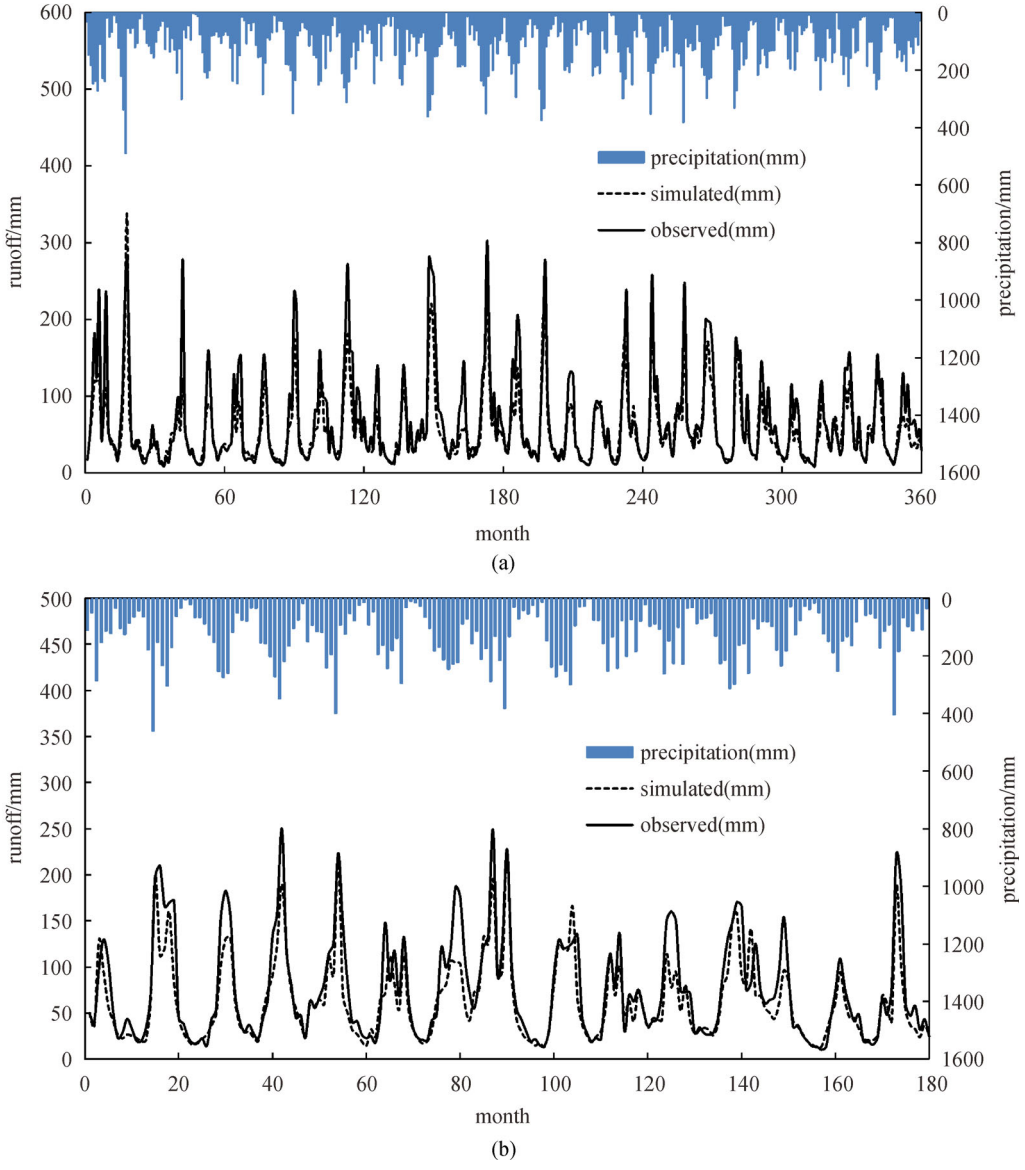

Fig. 5 Simulated and observed monthly runoff during calibration and verification periods at Waizhou Station in the Ganjiang sub-basin. (a) Calibration period (1961−1990). (b) Verification period (1991−2005).

estimated and observed monthly pan evaporation from 1961 to 2005 in the Ganjiang sub-basin are also shown in Fig. 6. The values of determination coefficient R^2 for all stations are over 0.8, which indicates that Eq. (11) is reasonable for estimating monthly evaporation in the study region. The downscaled temperature is transformed into projected evaporation series during future periods, which, together with downscaled precipitation, are used as inputs of the semi-distributed TPWBM to simulate future hydrologic changes compared with the historical period (1961–2005) in the Ganjiang sub-basin.

Table 4 demonstrates the projected future changes in annual mean precipitation, temperature, evaporation and runoff under three scenarios in the Ganjiang sub-basin. Evaporation increases throughout the next 90 years, following the warming trend in this basin. Annual average precipitation is projected to decrease under the RCP2.6 and RCP4.5 scenarios, and to increase under the RCP8.5 scenario. Annual runoff is projected to decrease in the 2020s and 2050s under all scenarios. In the 2080s, projected runoff is slightly less or more than that of historical periods under the RCP2.6 and RCP4.5 scenarios, while an increase of 13.7% is found under the RCP8.5 scenario. For the same period in the future, runoff increases with higher radiate forcing. For example, the projected annual mean runoff in the 2020s is 65.5 billion m^3 (BCM), 68.1 BCM, and 68.9 BCM under RCP2.6, RCP4.5 and RCP8.5, respectively.

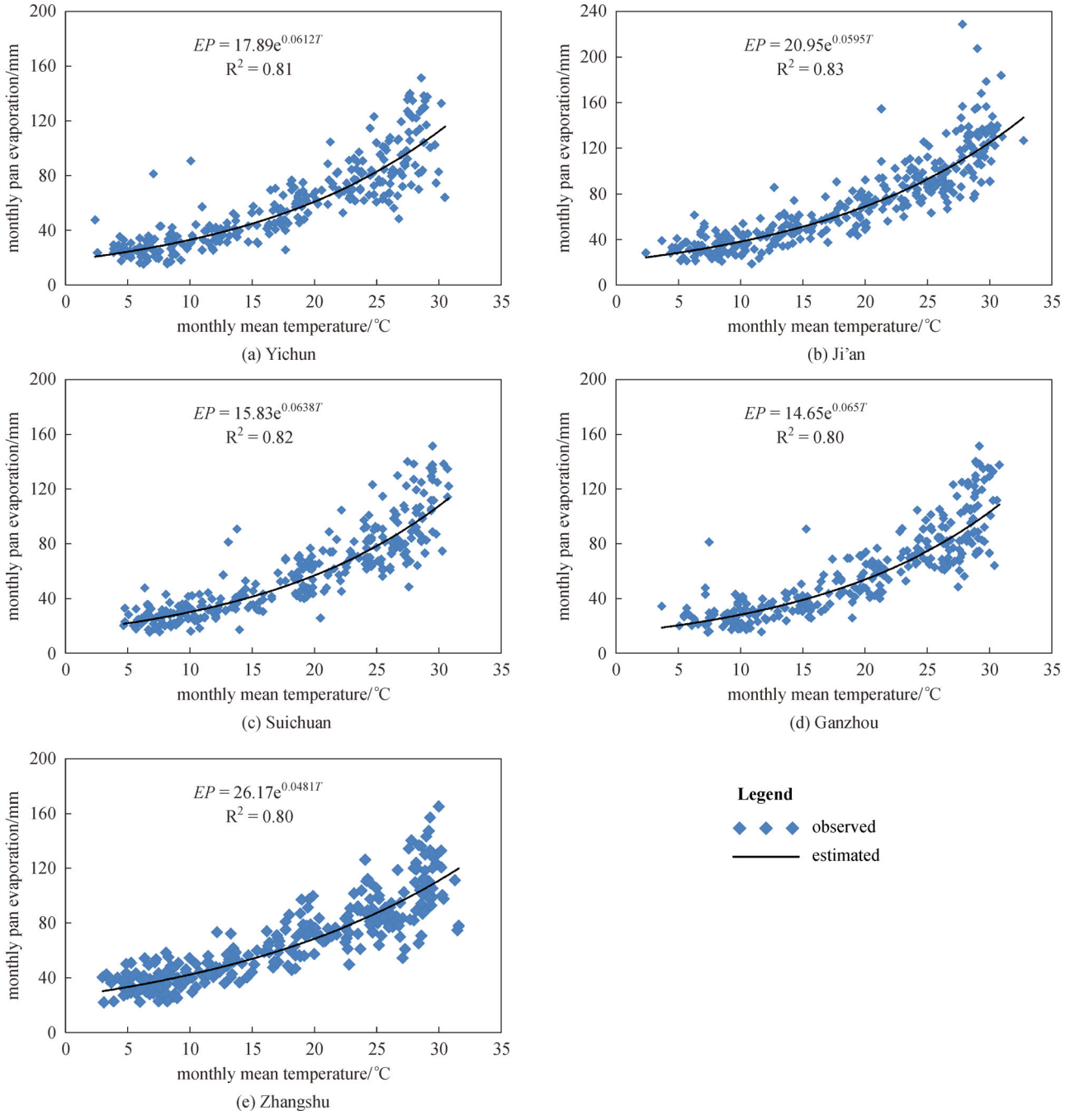

Fig. 6 Comparison of estimated and observed monthly pan evaporation at five meteorological stations in the Ganjiang sub-basin.

The relative changes in monthly precipitation, actual evaporation, and runoff under different RCPs in the future periods (2010−2099) are shown in Fig. 7. The projected changes in monthly precipitation, actual evaporation, and runoff under three scenarios for future periods in the Ganjiang sub-basin are analyzed and discussed. Combined with the results of Table 4, the amplitudes of precipitation variation are less than those of evaporation increments, leading to the amplification effect of decreasing runoff. In addition, there is a much larger difference in temporal distribution of precipitation within the year than that of evaporation, which indicates that the uneven changes in runoff in the temporal distributions is mainly influenced by uneven changes in precipitation. The results show that runoff in the Ganjiang sub-basin is more sensitive to changes in precipitation than evaporation.

Projected runoff changes during the main flood season (from April to June) and dry season (from September to March) under three scenarios in the Ganjiang sub-basin are shown in Fig. 8. Future runoff volume decreases in the

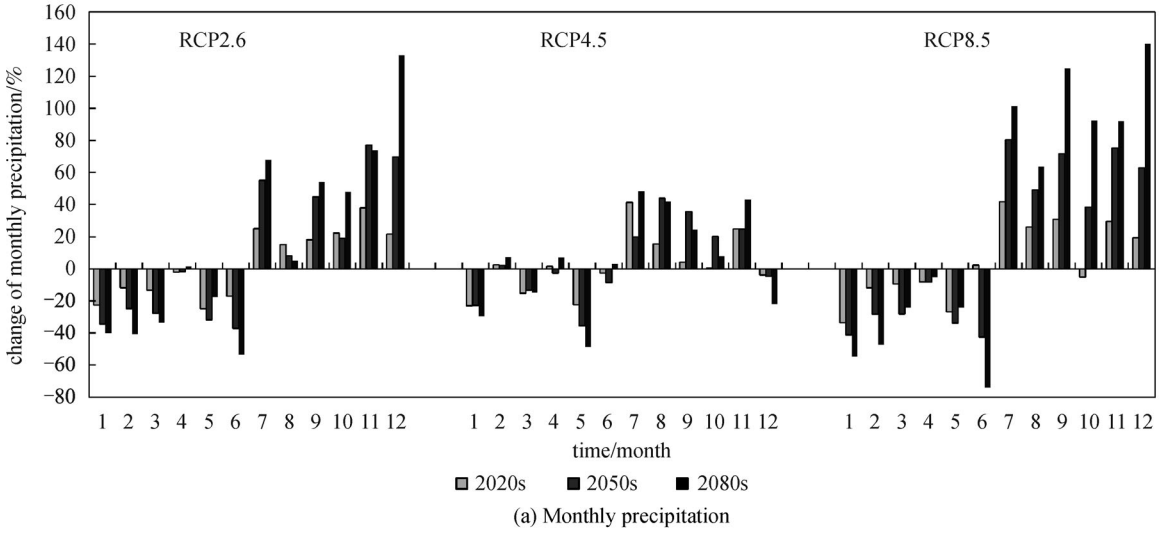

(a) Monthly precipitation

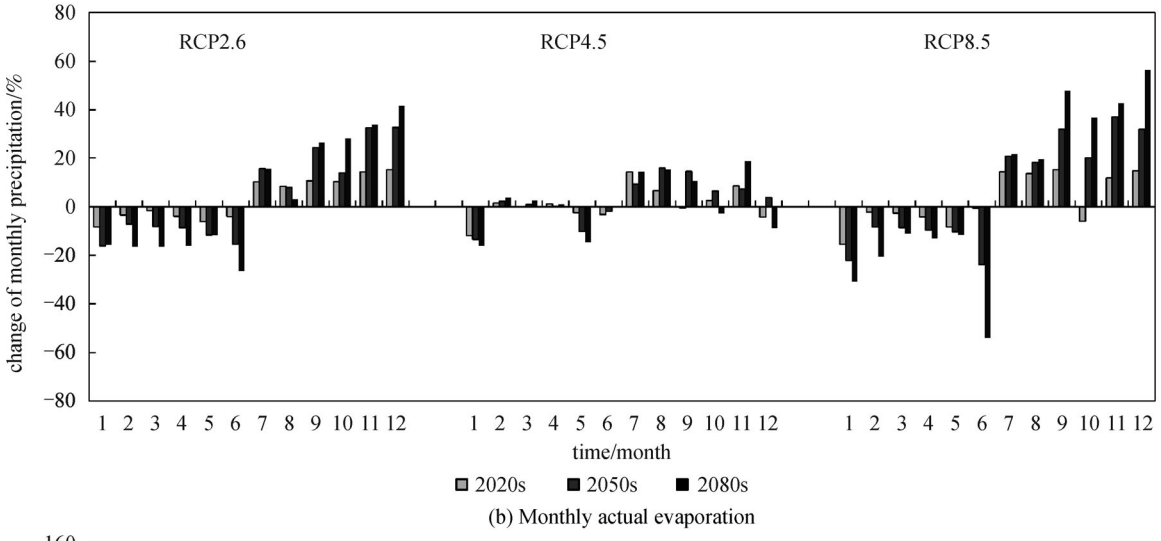

(b) Monthly actual evaporation

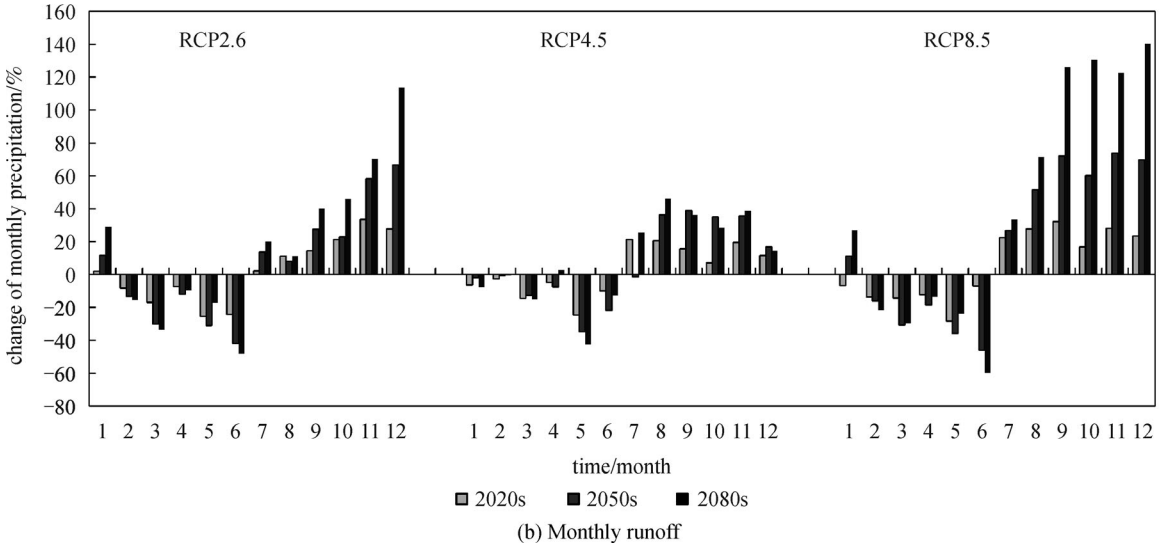

(b) Monthly runoff

Fig. 7 Relative changes of monthly precipitation, actual evaporation, and runoff under different RCPs in the future periods (2010–2099) in the Ganjiang sub-basin.

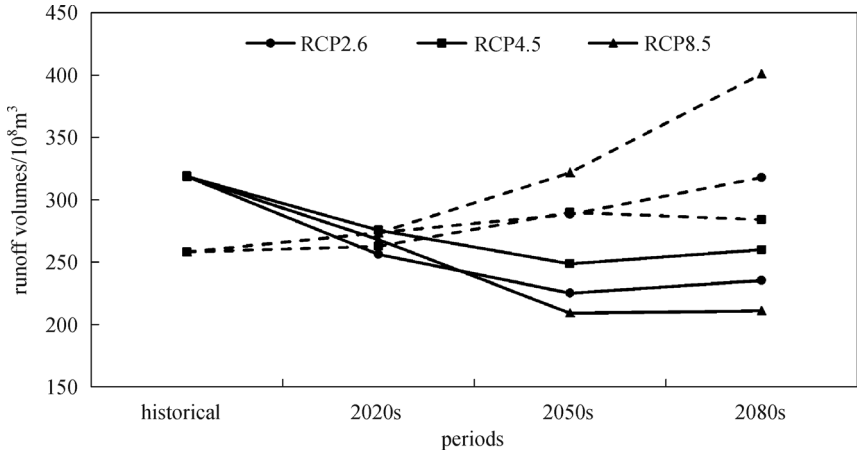

Fig. 8 Runoff changes during flood and dry seasons in the future periods (2010–2099) under different RCPs in the Ganjiang sub-basin. The solid and dashed lines represent runoff volume during flood and dry seasons, respectively.

Table 4 Projected future changes of annual mean precipitation, evaporation, and runoff in the Ganjiang sub-basin

Representative pathways	Variables	Historical periods	Future periods					
			2020s	Change/%	2050s	Change/%	2080s	Change/%
RCP2.6	*P*/mm	1538.2	1506.0	−2.09	1495.4	−2.78	1535.6	−0.17
	T/ºC	18.3	18.4	0.88	18.4	0.87	18.3	0.20
	E/mm	641.66	662.59	3.26	664.74	3.60	651.44	1.52
	W/(10^8 m^3)	695.32	655.32	−5.75	645.10	−7.22	690.64	−0.67
RCP4.5	*P*/mm	1538.2	1524.4	−0.90	1517.0	−1.38	1557.3	1.24
	T/ºC	18.3	18.5	1.03	18.7	2.31	18.7	2.41
	E/mm	641.66	654.88	2.06	665.93	3.78	662.65	3.27
	W/(10^8 m^3)	695.32	681.51	−1.99	675.26	−2.89	703.84	1.22
RCP8.5	*P*/mm	1538.2	1543.4	0.34	1546.9	0.56	1670.6	8.61
	T/ºC	18.3	18.5	1.06	18.7	2.53	19.0	4.15
	E/mm	641.66	663.74	3.44	676.82	5.48	667.88	4.09
	W/(10^8 m^3)	695.32	689.43	−0.85	694.49	−0.12	790.46	13.68

main flood season and increases in the dry season, indicating that climate change is likely to somewhat alleviate flood control pressure during the flood season and water supply pressure during the dry season.

5 Conclusions

The ever-increasing concentration of greenhouse gases in the Earth's atmosphere is projected to cause significant changes in hydrological patterns. To evaluate the hydrological response to climate change, projected changes of future runoff were simulated using a semi-distributed, two-parameter monthly water balance model in the Ganjiang sub-basin of Poyang Lake, China. The SDSM was used to downscale outputs of BCC-CSM1.1, recommended by the fifth phase of the CMIP5, under three scenarios (RCP2.6, RCP4.5, and RCP8.5) during future periods in the Poyang Lake Basin. The regional characteristics of future projections of mean precipitation and six extreme precipitation indices were analyzed. The main conclusions from this study are as follows:

1) The monthly mean precipitation was simulated reasonably well using SDSM with the NCEP reanalysis data and GCM outputs during the historical period (1961–2005). With bias-correction, SDSM can be applied to generate more reliable projections of extreme precipitation events in response to future climate change.

2) Projections indicate a mixed pattern of positive and/or negative changes in annual mean precipitation during future periods (2010–2099) in the Poyang Lake Basin. Six selected EPI demonstrate a general increase under the RCP4.5 and RCP8.5 scenarios, while no obvious trend was detected for most indices under the RCP2.6 scenario.

3) The future runoff in the Ganjiang sub-basin shows an overall decreasing trend under the RCP8.5 scenario, except

for the 2080s. Runoff is more sensitive to changes in precipitation than evaporation.

Findings shown in this paper provide an important scientific basis for the development of integrated watershed management measures for water security in Poyang Lake Basin.

Acknowledgements This study was supported by the National Nature Science Foundation of China (Grant Nos. 51539009 and 51190094), and the National Key Research and Development Plan of China (2016YFC0402206). The authors thank the editor and anonymous reviewers for their comments and suggestions, and Prof. Chong-Yu Xu and Dr. David E. Rheinheimer whose comments and English language editing helped to clarify and improve the quality of this paper.

References

Aich V, Liersch S, Vetter T, Huang S, Tecklenburg J, Hoffmann P, Koch H, Fournet S, Krysanova V, Müller E N, Hattermann F F (2014). Comparing impacts of climate change on streamflow in four large African river basins. Hydrol Earth Syst Sci, 18(4): 1305–1321

Alkama R, Marchand L, Ribes A, Decharme B (2013). Detection of global runoff changes: results from observations and CMIP5 experiments. Hydrol Earth Syst Sci, 17(7): 2967–2979

Arnell N W (2003). Effects of IPCC SRES* emissions scenarios on river runoff: a global perspective. Hydrol Earth Syst Sci, 7(5): 619–641

Bates B C, Kundzewicz Z W, Wu S,, Palutikof JP (eds)2008. Climate change and water. Technical Paper of the Intergovernmental Panel on Climate Change, IPCC Secretariat, Geneva, pp 15–18

Butts M B, Payne J T, Kristensen M, Madsen H (2004). An evaluation of the impact of model structure on hydrological modelling uncertainty for streamflow simulation. J Hydrol (Amst), 298(1−4): 242–266

Chen H, Guo S, Xu C, Singh V P (2007). Historical temporal trends of hydro-climatic variables and runoff response to climate variability and their relevance in water resource management in the Hanjiang basin. J Hydrol (Amst), 344(3−4): 171–184

Chen H, Xu C, Guo S (2012). Comparison and evaluation of multiple GCMs, statistical downscaling and hydrological models in the study of climate change impacts on runoff. J Hydrol (Amst), 434−435: 36–45

Christensen N S, Lettenmaier D P (2007). A multimodel ensemble approach to assessment of climate change impacts on the hydrology and water resources of the Colorado River Basin. Hydrol Earth Syst Sci, 11(4): 1417–1434

Chu J T, Xia J, Xu C, Singh V P (2010). Statistical downscaling of daily mean temperature, pan evaporation and precipitation for climate change scenarios in Haihe River, China. Theor Appl Climatol, 99(1−2): 149–161

Dibike Y B, Coulibaly P (2005). Hydrologic impact of climate change in the Saguenay watershed: comparison of downscaling methods and hydrologic models. J Hydrol (Amst), 307(1−4): 145–163

Easterling D R, Evans J L, Groisman P Y, Karl T R, Kunkel K E, Ambenje P (2000). Observed variability and trends in extreme climate events: a brief review. Bull Am Meteorol Soc, 81(3): 417–425

Fowler H J, Kilsby C G, Stunell J (2007). Modelling the impacts of projected future climate change on water resources in north-west England. Hydrol Earth Syst Sci, 11(3): 1115–1126

Frich P, Alexander L V, Della-Marta P, Gleason B, Haylock M, Klein Tank A M G, Peterson T (2002). Observed coherent changes in climatic extremes during the second half of the twentieth century. Clim Res, 19(3): 193–212

Gosling S N, Taylor R G, Arnell N W, Todd M C (2011). A comparative analysis of projected impacts of climate change on river runoff from global and catchment-scale hydrological models. Hydrol Earth Syst Sci, 15(1): 279–294

Guo J, Chen H, Xu C, Guo S, Guo J (2012). Prediction of variability of precipitation in the Yangtze River Basin under the climate change conditions based on automated statistical downscaling. Stochastic Environ Res Risk Assess, 26(2): 157–176

Guo J, Guo S, Li Y, Chen H, Li Y (2013). Spatial and temporal variation of extreme precipitation indices in the Yangtze River basin, China. Stochastic Environ Res Risk Assess, 27(2): 459–475

Guo S, Wang J, Xiong L, Ying A, Li D (2002). A macro-scale and semi-distributed monthly water balance model to predict climate change impacts in China. J Hydrol (Amst), 268(1−4): 1–15

Hanssen-Bauer I, Achberger C, Benestad R E, Chen D, Forland E J (2005). Statistical downscaling of climate scenarios over Scandinavia. Clim Res, 29(3): 255–268

Harpham C, Wilby R L (2005). Multi-site downscaling of heavy daily precipitation occurrence and amounts. J Hydrol (Amst), 312(1-4): 235–255

Hellström C, Chen D, Achberger C, Raisanen J (2001). Comparison of climate change scenarios for Sweden based on statistical and dynamical downscaling of monthly precipitation. Clim Res, 19(1): 45–55

Hong X, Guo S, Guo J, Hou Y, Wang L (2014). Projected changes of extreme precipitation characteristics in the Poyang Lake Basin based on statistical downscaling model. Journal of Water Resources Research, 3(6): 511–521 (in Chinese)

Houghton J T, Ding Y, Griggs D J, Noguer M, van der Linen P J, Dai X (2001). Climate Change 2001: the Scientific Basis. Cambridge: Cambridge University Press, 1–944

Huang A, Zhou Y, Zhang Y, Huang D, Zhao Y, Wu H (2014). Changes of the annual precipitation over central Asia in the twenty-first century projected by multimodels of CMIP5. J Clim, 27(17): 6627–6646

IPCC (2013). Climate Change 2013: the Physical Basis. Contribution of Working Group I to the Fifth Assessment Report of the IPCC. New York: Cambridge University Press

Islam S A, Bari M A, Anwar A H M F (2014). Hydrologic impact of climate change on Murray-Hotham catchment of Western Australia: a projection of rainfall–runoff for future water resources planning. Hydrol Earth Syst Sci, 18(9): 3591–3614

Jie M, Chen H, Xu C Y, Zeng Q, Tao X (2016). A comparative study of different objective functions to improve the flood forecasting accuracy. Hydrology Research, 47(4): 718–735

Kanai Y, Ueta M, Germogenov N, Nagendran M, Mita N, Higuchi H (2002). Migration routes and important resting areas of Siberian cranes (Grus leucogeranus) between northeastern Siberia and China as revealed by satellite tracking. Biol Conserv, 106(3): 339–346

Khan M S, Coulibaly P, Dibike Y (2006). Uncertainty analysis of

statistical downscaling methods. J Hydrol (Amst), 319(1-4): 357–382

Kwadijk J C J(1993) The impact of climate change on the discharge of the River Rhine, Ph.D. Thesis, Department of Physical Geography, Utrecht University, Netherlands Geographical Studies, 171.

Li J, Zhang Q, Chen Y D, Singh V P (2015). Future joint probability behaviors of precipitation extremes across China: spatiotemporal patterns and implications for flood and drought hazards. Global Planet Change, 124: 107–122

Li J, Zhang Q, Chen Y D, Xu C, Singh V P (2013). Changing spatiotemporal patterns of precipitation extremes in China during 2071–2100 based on Earth System Models. J Geophys Res, D, Atmospheres, 118(22): 12,537–12,555

Maraun D, Wetterhall F, Ireson A M, Chandler R E, Kendon E J, Widmann M, Brienen S, Rust H W, Sauter T, Themeßl M, Venema V K C, Chun K P, Goodness C M, Jones R G, Onof C, Vrac M, Thiele-Eich I (2010). Precipitation downscaling under climate change: recent developments to bridge the gap between dynamical models and the end users. Rev Geophys, 48(3): 1–38

Merritt W S, Alila Y, Barton M, Taylor B, Cohen S, Neilsen D (2006). Hydrologic response to scenarios of climate change in sub-watersheds of the Okanagan basin, British Columbia. J Hydrol (Amst), 326(1-4): 79–108

Middelkoop H, Daamen K, Gellens D, Grabs W, Kwadijk J C J, Lang H, Parmet B W A H, Schädler B, Schulla J, Wilke K (2001). Impact of climate change on hydrological regimes and water resources management in the Rhine basin. Clim Change, 49(1/2): 105–128

Moss R H, Edmonds J A, Hibbard K A, Manning M R, Rose S K, van Vuuren D P, Carter T R, Emori S, Kainuma M, Kram T, Meehl G A, Mitchell J F B, Nakicenovic N, Riahi K, Smith S J, Stouffer R J, Thomson A M, Weyant J P, Wilbanks T J (2010). The next generation of scenarios for climate change research and assessment. Nature, 463(7282): 747–756

Penman H L (1948). Natural evaporation from open water, bare soil and grass. Proc R Soc Lond, 193(1032): 120–145

Peterson T C, Taylor M A, Demeritte R, Duncombe D L, Burton S, Thompson F, Porter A, Mercedes M, Villegas E, Fils R S, Tank A K, Martis A,Warner R, Joyette A, Mills W, Alexander L, Gleason B (2002). Recent changes in climate extremes in the Caribbean region. Journal of Geophysical Research: Atmospheres (1984–2012), 107 (D21): ACL 16-1–ACL 16-9

Plummer N, Salinger M J, Nicholls N, Suppiah R, Hennessy K J, Leighton R M, Trewin B, Page C M, Lough J M (1999). Twentieth century trends in climate extremes over the Australian region and New Zealand. Clim Change, 42(1): 183–202

Priestley C H B, Taylor R J (1972). On the assessment of surface heat flux and evaporation using large-scale parameters. Mon Weather Rev, 100(2): 81–92

Qian W, Lin X (2005). Regional trends in recent precipitation indices in China. Meteorol Atmos Phys, 90(3−4): 193–207

Raje D, Krishnan R (2012). Bayesian parameter uncertainty modeling in a macro-scale hydrologic model and its impact on Indian river basin hydrology under climate change. Water Resour Res, 48(8): W08522

Refsgaard J C, Havnø K, Ammentorp H C, Verwey A (1988). Application of hydrological models for flood forecasting and flood control in India and Bangladesh. Adv Water Resour, 11(2): 101–105

Sen Roy S, Balling R C (2004). Trends in extreme daily precipitation indices in India. Int J Climatol, 24(4): 457–466

Shabalova M V, Van Deursen W P A, Buishand T A (2003). Assessing future discharge of the river Rhine using regional climate model integrations and a hydrological model. Clim Res, 23(3): 233–246

Shankman D, Keim B D, Song J (2006). Flood frequency in China's Poyang Lake region: trends and teleconnections. Int J Climatol, 26 (9): 1255–1266

Sillmann J, Kharin V V, Zwiers F W, Zhang X, Bronaugh D (2013). Climate extremes indices in the CMIP5 multimodel ensemble: Part 2. Future climate projections. J Geophys Res, D, Atmospheres, 118(6): 2473–2493

Sun S, Chen H, Ju W, Yu M, Hua W, Yin Y (2014). On the attribution of the changing hydrological cycle in Poyang Lake Basin, China. J Hydrol (Amst), 514: 214–225

Tao H, Fraedrich K, Menz C, Zhai J (2014). Trends in extreme temperature indices in the Poyang Lake Basin, China. Stochastic Environ Res Risk Assess, 28(6): 1543–1553

Taylor K E, Stouffer R J, Meehl G A (2012). An overview of CMIP5 and the experiment design. Bull Am Meteorol Soc, 93(4): 485–498

Teutschbein C, Seibert J (2010). Regional climate models for hydrological impact studies at the catchment scale: a review of recent modeling strategies. Geogr Compass, 4(7): 834–860

Thibeault J M, Seth A (2014). Changing climate extremes in the Northeast United States: observations and projections from CMIP5. Clim Change, 127(2): 273–287

Thornthwaite C W (1948). An approach toward a rational classification of climate. Geogr Rev, 38(1): 55–94

Wang G, Zhang J, Li Y, Bao Z, Jin J, Yan X, Liu C (2014). Variation trend of future climate for the Hai River Basin based on multiple GCMs projections. Resources Science, 36(5): 1043–1050 (in Chinese with English abstract)

Wetterhall F, Bárdossy A, Chen D, Halldin S, Xu C (2006). Daily precipitation downscaling techniques in three Chinese regions. Water Resour Res, 42(11): W11423

Widén-Nilsson E, Halldin S, Xu C Y (2007). Global water-balance modelling with WASMOD-M: parameter estimation and regionalization. J Hydrol (Amst), 340(1-2): 105–118

Wilby R L, Dawson C W, Barrow E M (2002). SDSM- a decision support tool for the assessment of regional climate change impacts. Environ Model Softw, 17(2): 145–157

Wilby R L, Hay L E, Leavesley G H (1999). A comparison of downscaled and raw GCM output: implications for climate change scenarios in the San Juan River basin, Colorado. J Hydrol (Amst), 225(1−2): 67–91

Wilby R L, Tomlinson O J, Dawson C W (2003). Multi-site simulation of precipitation by conditional resampling. Clim Res, 23(3): 183–194

Wilby R L, Wigley T M L, Conway D, Jones P D, Hewitson B C, Main J, Wilks D S (1998). Statistical downscaling of general circulation model output: a comparison of methods. Water Resour Res, 34(11): 2995–3008

Wilks D S (1989). Conditioning stochastic daily precipitation models on total monthly precipitation. Water Resour Res, 25(6): 1429–1439

Xin X, Wu T, Li J, Wang Z, Li W, Wu F (2013). How well does BCC_CSM1. 1 reproduce the 20th century climate change over China? Atmospheric and Oceanic Science Letters, 6(1): 21–26

Xiong L, Guo S (1999). A two-parameter monthly water balance model and its application. J Hydrol (Amst), 216(1-2): 111–123

Xu C-Y (1999). From GCMs to river flow: a review of downscaling methods and hydrologic modelling approaches. Prog Phys Geogr, 23 (2): 229–249

Xu C-Y, Singh V P (2001). Evaluation and generalization of temperature-based methods for calculating evaporation. Hydrol Processes, 15(2): 305–319

Xu C-Y, Widén E, Halldin S (2005). Modelling hydrological consequences of climate change- progress and challenges. Adv Atmos Sci, 22(6): 789–797

Xu Y, Xu C, Gao X, Luo Y (2009). Projected changes in temperature and precipitation extremes over the Yangtze River basin of China in the 21st century. Quat Int, 208(1-2): 44–52

Ye X, Li Y, Li X, Xu C-Y, Zhang Q (2015). Investigation of the variability and implications of meteorological dry/wet conditions in the Poyang Lake catchment, China, during the period 1960−2010. Adv Meteorol, 2015: 1–11

Ye X, Liu J, Li X, Zhang Q (2013). Effects of climate variability and human activities on runoff variation of Ganjiang river basin. Journal of Hohai University (Natural Sciences), 41(3): 196–203 (in Chinese with English abstract)

Ye X, Zhang Q, Bai L, Hu Q (2011). A modeling study of catchment discharge to Poyang Lake under future climate in China. Quat Int, 244(2): 221–229

Zhang Q, Liu Y, Yang G, Zhang Z (2011a). Precipitation and hydrological variations and related associations with large-scale circulation in the Poyang Lake Basin, China. Hydrol Processes, 25 (5): 740–751

Zhang Q, Sun P, Chen X, Jiang T (2011b). Hydrological extremes in the Poyang Lake Basin, China: changing properties, causes and impacts. Hydrol Processes, 25(20): 3121–3130

Zhang Q, Xiao M, Li J, Singh V P, Wang Z (2014a). Topography-based spatial patterns of precipitation extremes in the Poyang Lake Basin, China: Changing properties and causes. J Hydrol (Amst), 512: 229–239

Zhang Q, Xiao M, Singh V P, Chen Y D (2014b). Max-stable based evaluation of impacts of climate indices on extreme precipitation processes across the Poyang Lake Basin, China. Global Planet Change, 122: 271–281

Zhang X, Yang F (2004). RClimDex (1.0) user manual. Climate Research Branch Environment, Canada, pp22